Random site percolation thresholds on square lattice for complex neighborhoods containing sites up to the sixth coordination zone

Krzysztof Malarz[*]

AGH University, Faculty of Physics and Applied Computer Science, al. Mickiewicza 30, 30-059 Kraków, Poland
(Dated: October 23, 2023)

The site percolation problem is one of the core topics in statistical physics. Evaluation of the percolation threshold, which separates two phases (sometimes described as conducting and insulating), is useful for a range of problems from core condensed matter to interdisciplinary application of statistical physics in epidemiology or other transportation or connectivity problems. In this paper with Newman–Ziff fast Monte Carlo algorithm and finite-size scaling theory the random site percolation thresholds p_c for a square lattice with complex neighborhoods containing sites from the sixth coordination zone are computed. Complex neighborhoods are those that contain sites from various coordination zones (which are not necessarily compact). We also present the source codes of the appropriate procedures (written in C) to be replaced in original Newman–Ziff code. Similar to results previously found for the honeycomb lattice, the percolation thresholds for complex neighborhoods on a square lattice follow the power law $p_c(\zeta) \propto \zeta^{-\gamma_2}$ with $\gamma_2 = 0.5454(60)$, where $\zeta = \sum_i z_i r_i$ is the weighted distance of sites in complex neighborhoods (r_i and z_i are the distance from the central site and the number of sites in the coordination zone i, respectively).

Keywords: Monte Carlo simulation; finite-size scaling; non-compact neighborhoods; universal formula for percolation thresholds

I. INTRODUCTION

Percolation [1, 2] is one of the core problems in statistical physics with many interdisciplinary applications ranging from materials science [3], through studies of polymer composites [4], forest fires [5], agriculture [6], oil and gas exploration [7], diseases propagation [8], transportation networks [9], quantifying urban areas [10], to Bitcoins transfer [11] (see References 12 and 13 for reviews). The percolating system undergoes a (purely geometrical) phase transition (in terms of the conductivity or transportation properties of the system) from the phase corresponding to an insulator (for low connectivity $p < p_c$) to a conductor (for high connectivity $p > p_c$). The critical connectivity of the system p_c (called the percolation threshold) separates these two phases and depends on the dimension of the system d, the topology of the lattice, the number z of sites in the assumed neighborhood, the type of percolation (that is, the site or bond dilution), etc. [14, 15].

Percolation thresholds were initially estimated for nearest-neighbor interactions [16–18] but later also complex neighborhoods (termed also extended for compact neighborhoods) were studied for various lattices embedded in:

- $d = 2$ (for a square [19–25], a triangular [19, 20, 26–28], a honeycomb [19, 29] and other Archimedean [30, 31] lattices);

- $d = 3$ (for a simple cubic [25, 32, 33] lattice);

- $d = 4$ (for a simple hypercubic [34, 35] lattice)

dimensions.

Simultaneously with the estimation of percolation thresholds for various lattices, some effort went into searching for an analytical formula allowing for the prediction of the percolation threshold position based on lattice characteristics. For example, Xun *et al.* [31] estimated the site and bond percolation thresholds for 11 Archimedean lattices with complex and compact (extended) neighborhoods containing sites up to the tenth coordination zone. For the site percolation problem, the critical site occupation probability p_c follows asymptotically

$$p_c(z) = a/z \tag{1}$$

with the total number z of sites in the neighborhood and $a \approx 4.51235$. This dependence should be reached exactly for the percolation of compact neighborhoods with a large number z of sites that make up the neighborhood (for example, for discs). To take into account finite-z effect an additional term b in the denominator of Equation (1)

$$p_c(z) = c/(z + b) \tag{2}$$

has been included [36]. For the two-dimensional lattices $b = 3$ [31]. The third universal scaling studied in by Xun *et al.* [31] was

$$p_c(z; d) = 1 - \exp(d/z) \tag{3}$$

proposed by Koza *et al.* [37, 38].

Much earlier Galam and Mauger [39, 40] proposed a universal formula for site percolation problem

$$p_c(z; d) = \frac{p_0}{[(d-1)(z-1)]^a}. \tag{4}$$

They recognized two classes of systems (two sets of (p_0, a) parameters) [39]. Their paper [39] was immediately criticized by van der Marck [41] who showed 'an example of
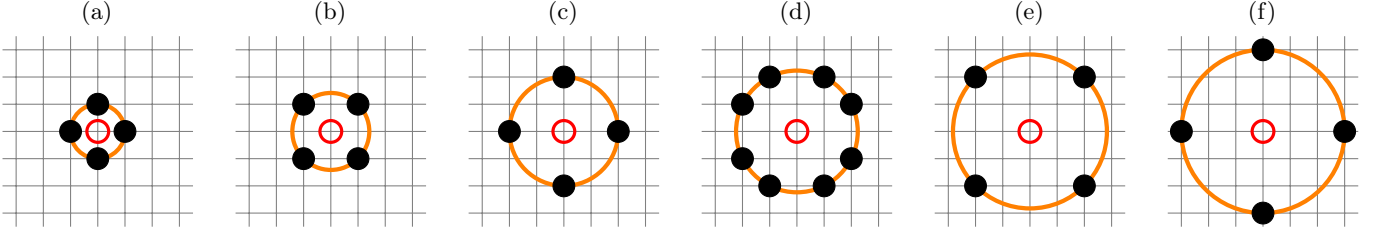

FIG. 1: Shapes of basic neighborhoods on square lattice. (a) SQ-1, $r^2 = 1$, (b) SQ-2, $r^2 = 2$, (c) SQ-3, $r^2 = 4$, (d) SQ-4, $r^2 = 5$, (e) SQ-5, $r^2 = 8$, (f) SQ-6, $r^2 = 9$. The number r is the radius of (orange) circle indicating equidistant sites marked by solid (black) circles to the central one marked with open (red) circle

two networks, where d and z are equal, but the percolation thresholds differ'.

For complex neighborhoods, the situation is even more complex, since for a given lattice topology (and thus fixed d) there are many neighborhoods with exactly the same total number z of sites in the neighborhood but different percolation thresholds p_c (see: Table 1 and Figure 4 in Reference 24 for the square lattice; Table 1 in Reference 27 and Table 1 and Figure 3(a) in Reference 28 for the triangular lattice; and Table 1 and Figure 4(a) in Reference 29 for the honeycomb lattice).

To solve the above-mentioned problems of $p_c(z)$ degeneration the index

$$\xi = \sum_i z_i r_i^2 / i \qquad (5)$$

was proposed by Malarz [28]. The z_i and r_i are the number of sites and their distance from the central site in the neighborhood in the i-th coordination zone. The index ξ allowed for a successful distinguishing between neighborhoods and cancel $p_c(z)$ degeneration for the triangular lattice with complex neighborhoods containing sites up to the fifth coordination zone. The dependence of the percolation threshold

$$p_c(\xi) \propto \xi^{-\gamma_1} \qquad (6)$$

was well fitted with the power law with $\gamma_1(\text{TR}) \approx 0.710(19)$. Unfortunately, this dependence does not hold for the honeycomb lattice (see Figure 4(b) in Reference 29). Thus, another index

$$\zeta = \sum_i z_i r_i \qquad (7)$$

was introduced by Malarz, to simultaneously resolve the problem of $p_c(z)$ degeneration and to distinguish among various complex neighborhoods for the honeycomb lattice [29]. For honeycomb lattice and complex neighborhoods up to the fifth coordination zone

$$p_c(\zeta) \propto \zeta^{-\gamma_2} \qquad (8)$$

with $\gamma_2(\text{HC}) \approx 0.4981(90)$ [29].

In this paper, using the fast Monte Carlo Newman–Ziff algorithm [42], we calculate the critical occupation probabilities p_c (percolation thresholds) for random site percolation in a square lattice and neighborhoods combined with basic neighborhoods presented in Figure 1. The basic neighborhoods contain sites from the first coordination zone (SQ-1, Figure 1(a)) up to the sixth coordination zone (SQ-6, Figure 1(f)). These complex neighborhoods are presented in Figure 4 in Appendix A. Calculations of percolation thresholds are based on the finite-size scaling hypothesis [14, 43, 44].

The second aim of this paper is to check if Equations (6) and (8) holds for a square lattice with complex neighborhoods and, if so, which of them performs better.

The rest of the paper is organized as follows. The details of the calculations are presented in the following Section II. The results of the calculations are given in Section III. The article is summarized and concluded in Section V. The Appendix A contains graphical presentation of neighborhood shapes. In "Supplementary materials" we present:

- a set of `boundaries()` functions (written in C, Listings 1 to 6) to be replaced in the Newman–Ziff program published in Reference 42 to obtain the single realization of $\mathcal{S}_{\max}(n; L)$ for the neighborhoods presented in Figures 1(a) to 1(f);

- and the dependencies of $\mathcal{P}_{\max} \cdot L^{\beta/\nu}$ on the probability of occupation p for neighborhoods ranging from SQ-6 to SQ-1,2,3,4,5,6 for various linear system sizes $L = 128$ to 4096.

II. COMPUTATIONS

Our calculations of the percolation thresholds p_c are based on finite-size analyses of the probability $\mathcal{P}_{\max}$ that the randomly selected site belongs to the largest cluster of occupied sites. According to the finite-size hypothesis [14, 43, 44], in the vicinity of a phase transition (marked by a critical point x_c), many quantity $\mathcal{A}$ characterizing the system obeys a scaling relation

$$\mathcal{A}(x; L) = L^{-\varepsilon_1} \mathcal{F}\left((x - x_c)L^{\varepsilon_2}\right), \qquad (9)$$

where x measures the level of system disorder (temperature for the Ising or Potts model, site/bond occupation probability for percolation problem), L is the linear size of the system, $\mathcal{F}$ is a scaling function (usually analytically unknown) and ε_1 and ε_2 are scaling exponents. In other words, there exists a function $\mathcal{F}$, that for properly assumed values of x_c, ε_1 and ε_2 the dependencies of $\mathcal{A}(x)$ collapse into a single curve independently of the (finite) system size L. This also provides an elegant way to predict the value of the critical parameter x_c as

$$\mathcal{A}(x;L)L^{\varepsilon_1} = \mathcal{F}\left((x - x_c)L^{\varepsilon_2}\right), \tag{10}$$

which for $x = x_c$ yields

$$\mathcal{A}(x_c;L)L^{\varepsilon_1} = \mathcal{F}(0). \tag{11}$$

In other words, we expect the curves $L^{\varepsilon_1}\mathcal{A}(x)$ plotted for various sizes of linear systems L to intercept each other at $x = x_c$.

For our purposes, we assume that $\mathcal{A} \equiv \mathcal{P}_{\max}$ (the probability that a randomly selected site belongs to the largest cluster) and $x \equiv p$ (the probability of occupation of the sites). For the problem of site percolation, the critical values of the exponents ε_1 and ε_2 are known exactly [14, p. 54] as $\varepsilon_1 = \frac{5}{36}/\frac{4}{3} = \frac{5}{48}$ and $\varepsilon_2 = 1/\frac{4}{3} = \frac{3}{4}$.

To compute the probability of belonging to the largest cluster

$$\mathcal{P}_{\max}(p;L) = \mathcal{S}_{\max}(p;L)/N \tag{12}$$

we first need to calculate the sizes of the largest cluster $S_{\max}$ and $N = L^2$ is the number of all sites available in the system.

To that end, we use three concepts presented in Reference 42.

- The first is the fast system construction scheme (known as the Newman–Ziff algorithm). The efficiency of this approach is based on the recursive construction of the system with n occupied sites with the addition of only one occupied site to the system containing $(n-1)$ already occupied sites.

- The second concept is the way of transforming the $\bar{\mathcal{A}}(n;N)$ dependence on the integer number of occupied sites n into the dependence $\mathcal{A}(p;N)$ on the probability of the site occupation p

$$\mathcal{A}(p;N) = \sum_{n=0}^{N} \bar{\mathcal{A}}(n;N)\mathcal{B}(n;N,p), \tag{13}$$

where

$$\mathcal{B}(n;N,p) = \binom{N}{n}p^n(1-p)^{N-n} \tag{14}$$

are values of the binomial (Bernoulli) probability distribution.

- The third concept is the efficient construction of the binomial coefficients (14).

The applied scheme defined in Equation (13) together with the construction of the binomial distribution coefficients is presented in Algorithm 1.

Algorithm 1 Conversion $\bar{\mathcal{A}}(n)$ to $\mathcal{A}(p)$ [42]

Require: p_1, p_2, Δp, N, $\bar{\mathcal{A}}(n)$ $\quad \triangleright n \in \{0,1,\cdots,N-1,N\}$
Ensure: $\mathcal{A}(p)$ $\quad\quad\quad \triangleright$ for p from p_1 to p_2 every Δp
1: $p \leftarrow p_1$
2: **while** $p \leq p_2$ **do**
3: $\quad n_{\max} = pN$ $\quad\quad\quad\quad \triangleright$ store $\mathcal{B}(N,n,p)$ to $\hat{B}$
4: $\quad B(n_{\max}) = pN$
5: $\quad$ **for** $n = n_{\max} + 1, N$ **do**
6: $\quad\quad B(n) = B(n-1) \cdot \dfrac{(N-n+1)p}{n(1-p)}$
7: $\quad$ **end for**
8: $\quad$ **for** $n = n_{\max} - 1, 0, -1$ **do**
9: $\quad\quad B(n) = B(n+1) \cdot \dfrac{(n+1)(1-p)}{p(N-n)}$
10: $\quad$ **end for**
11: $\quad c \leftarrow \sum \hat{B}$
12: $\quad \hat{B} \leftarrow \hat{B}/c$
13: $\quad \mathcal{A}(p) = 0$
14: $\quad$ **for all** n **do**
15: $\quad\quad \mathcal{A}(p) \leftarrow \mathcal{A}(p) + B(n)\bar{\mathcal{A}}(n)$
16: $\quad$ **end for**
17: $\quad$ **return** $p, \mathcal{A}(p)$
18: $\quad p \leftarrow p + \Delta p$
19: **end while**

III. RESULTS

In Figure 2 examples of the results (for neighborhood SQ-1,2,3,4,5,6 and various sizes of linear systems $L = 128$, 256, 512, 1024, 2048, and 4096) of the computations obtained with the procedure described in Section II are presented. Figure 2(a) shows dependencies of the largest cluster size $\mathcal{S}_{\max}$ (normalized to the system size L^2) vs. the number of occupied sites n (also normalized to the system size L^2). With increasing system linear size L the dependence $\mathcal{S}_{\max}(n)$ becomes steeper and steeper. Figure 2(b) shows $L^{\varepsilon_1}\mathcal{P}_{\max}(p)$ for p ranging from 0.134 to 0.152 estimated for every $\Delta p = 10^{-4}$. Figure 2(c) shows close-up of Figure 2(b) in the vicinity of the percolation threshold (for p from 0.1430 to 0.1435 for every $\Delta p = 10^{-5}$). The finite-size effects in $L^{\varepsilon_1}\mathcal{P}_{\max}(p)$ vanish for $p = p_c$, resulting in a common point of $L^{\varepsilon_1}\mathcal{P}_{\max}(p)$ plotted for various linear sizes L of the systems. The analogous dependencies for all other complex neighborhoods—presented in Figure 4 in Appendix A—containing sites from the sixth coordination zone are shown in Figure 5. The results are averaged over the realizations of the $R = 10^5$ system. The obtained p_c are gathered in Table I.

In Figure 3 the dependencies of p_c on the total number $z = \sum_i z_i$ of sites in the complex neighborhoods containing the sites of the i-th coordination zone and the indexes ξ and ζ are presented. Figure 3(a) shows the dependence of the percolation threshold p_c on z. The per-
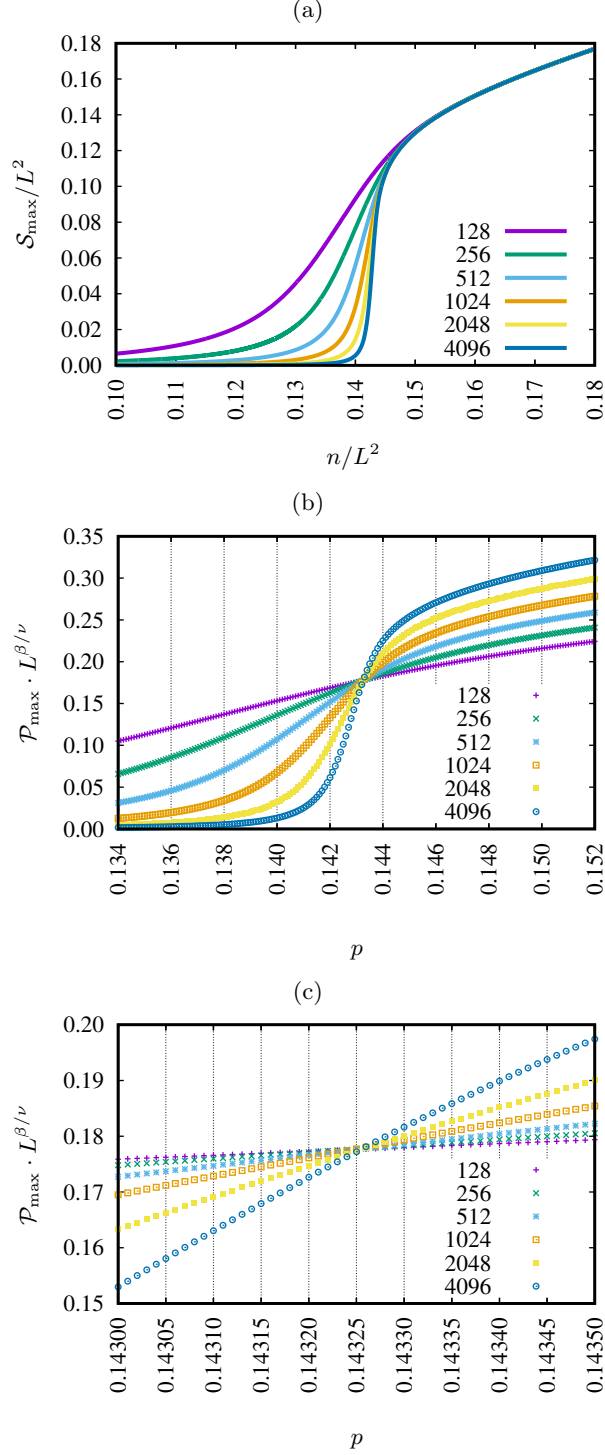
FIG. 2: An example of results obtained for
sq-1,2,3,4,5,6 neighborhood and various linear system
sizes $L = 128$ to 4096. (a) The size of the largest cluster
$\mathcal{S}_{\max}$ vs. the number of occupied sites n. Both
quantities are normalized to the system size L^2. (b)
Dependence of $L^{\varepsilon_1}\mathcal{P}_{\max}(p)$ for p from 0.134 to 0.152
every $\Delta p = 10^{-4}$. (c) Close-up on Figure 2(b) in the
vicinity of the percolation threshold p_c for p from
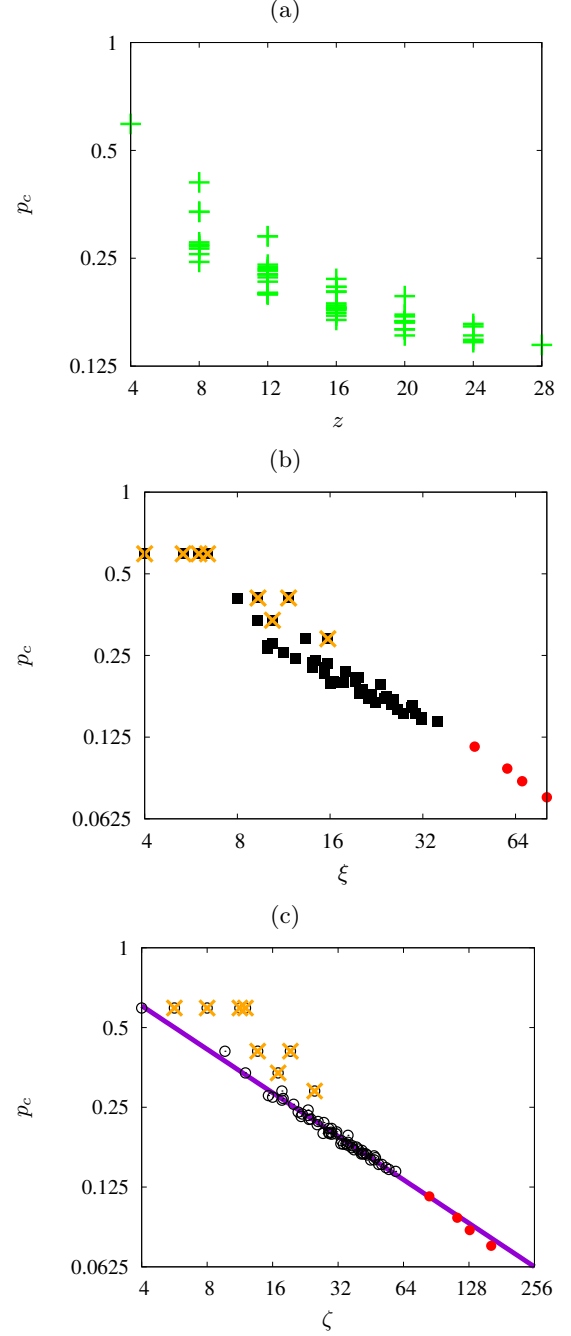0.1430 to 0.1435 every $\Delta p = 10^{-5}$

FIG. 3: (a) Degeneracy of $p_c(z)$ for a square lattice with
complex neighborhoods ranging from sq-1 up to
sq-1,2,3,4,5,6. (b) Dependence $p_c(\xi)$ for various
neighborhoods containing sites up to the sixth
coordination zone. Orange crosses show equivalent
neighborhoods (sq-1≡sq-2≡sq-3≡sq-5≡sq-6,
sq-1,3≡sq-2,5, sq-1,2≡sq-2,3≡sq-3,5 and
sq-1,2,3≡sq-2,3,5). (c) Dependence $p_c(\zeta)$. Inflated
neighborhoods corresponding to higher indexes (i.e.,
sq-2, sq-3, sq-5, sq-6, sq-2,5, sq-2,3, sq-3,5 and
sq-2,3,5) are excluded from the fitting procedure. The
solid (violet) line indicates Equation (8) with
$\gamma_2(\text{sq}) = 0.5454(60)$

TABLE I: Percolation thresholds p_c for a square lattice with complex neighborhoods (and their characteristics z, ζ, ξ) containing sites from the sixth coordination zone

lattice	z	ζ	ξ	p_c
sq-1,2,3,4,5,6	28	58.8591	35.7333	0.14326[a]
sq-2,3,4,5,6	24	54.8591	31.7333	0.14575
sq-1,3,4,5,6	24	53.2023	31.7333	0.14801
sq-1,2,4,5,6	24	50.8591	30.4	0.15223
sq-1,2,3,5,6	20	40.9706	25.7333	0.16661
sq-1,2,3,4,6	24	47.5454	29.3333	0.16134
sq-3,4,5,6	20	49.2023	27.7333	0.15221
sq-2,4,5,6	20	46.8591	26.4	0.15844
sq-2,3,5,6	16	36.9706	21.7333	0.17601
sq-2,3,4,6	20	43.5454	25.3333	0.16529
sq-1,4,5,6	20	45.2023	26.4	0.15815
sq-1,3,5,6	16	35.3137	21.7333	0.18007
sq-1,3,4,6	20	41.8885	25.3333	0.16675
sq-1,2,5,6	16	32.9706	20.4	0.18216
sq-1,2,4,6	20	39.5454	24	0.17409
sq-1,2,3,6	16	29.6569	19.3333	0.20134
sq-4,5,6	16	41.2023	22.4	0.16819
sq-3,5,6	12	31.3137	17.7333	0.19867
sq-3,4,6	16	37.8885	21.3333	0.17288
sq-2,5,6	12	28.9706	16.4	0.20036
sq-2,4,6	16	35.5454	20	0.18454
sq-2,3,6	12	25.6569	15.3333	0.21503
sq-1,5,6	12	27.3137	16.4	0.19936
sq-1,4,6	16	33.8885	20	0.18143
sq-1,3,6	12	24	15.3333	0.22577
sq-1,2,6	12	21.6569	14	0.23076
sq-5,6	8	23.3137	12.4	0.24422
sq-4,6	12	29.8885	16	0.19799
sq-3,6	8	20	11.3333	0.25673
sq-2,6	8	17.6569	10	0.26600
sq-1,6	8	16	10	0.27309
sq-6[b]	4	12	6	0.59274[c]

[a] 0.142 [26], 0.143255 [25]

[b] equivalent to sq-1

[c] 0.592746 [14, p. 17], 0.59274621(13) [45], 0.59274(5) [46] for sq-1

colation thresholds for neighborhoods containing sites up to the fifth coordination zone are taken from References 22 and 24 and those for neighborhoods containing sites from the sixth coordination zone presented here in Table I. It is clear that z cannot differentiate between the various shapes of the neighborhoods or the percolation thresholds associated with them.

In Figure 3(b) the dependence (6) on the percolation threshold p_c for complex neighborhoods on the square lattice on the index ξ is presented. Similarly to the earlier observation for the honeycomb lattice [29], some deviations from the straight line in Equation (6) are observed. The full circles mark percolation thresholds for compact neighbourhoods sq-1,2,$\cdots$,6,7, sq-1,2,$\cdots$,7,8, sq-1,2,$\cdots$,8,9 and sq-1,2,$\cdots$,9,10) taken from References 25 and 26.

Figure 3(c) shows the dependence (8) of p_c for complex neighborhoods on the square lattice on the index ζ. The percolation thresholds for neighborhoods containing sites up to the fifth coordination zone are taken from References 22 and 24, those for neighborhoods containing sites from the sixth coordination zone presented here in Table I and those for compact neighborhoods containing sites from the seventh to the tenth coordination zones are taken from References 25 and 26.

IV. DISCUSSION

The percolation thresholds p_c obtained in simulations range from 0.59275 (for sq-6) to 0.14325 (for sq-1,2,3,4,5,6). The latter agrees in five significant digits with its earlier estimate $p_c(\text{sq-1,2,3,4,5,6}) = 0.143255$ [25]. The sq-6 neighborhood is topologically equivalent to sq-1 (but for a three-times larger lattice constant), resulting in identical percolation thresholds $p_c(\text{sq-6}) = p_c(\text{sq-1})$. For the sq-6 neighborhood we deal with several simultaneous independent percolation problems on several identically shaped lattices. The latter reduces effective system size, but our results show, that this effect is perfectly compensated by effective increase of number of samples.

Similarly to the honeycomb lattice [29], the power law (8) also holds for a square lattice with complex neighborhoods with $\gamma_2(\text{sq}) = 0.5454(60)$ given by the least-squares method. Inflated neighborhoods sq-2, sq-3, sq-5, sq-6, sq-2,3, sq-3,5, sq-2,5 and sq-2,3,5 (corresponding to sq-1, sq-1, sq-1, sq-1, sq-1,2, sq-1,2, sq-1,3 and sq-1,2,3, respectively) were excluded from the fitting procedure.

Among the neighborhoods that contain sites up to the sixth coordination zone, there are seven pairs of various neighborhoods with exactly the same ζ index, namely $\zeta(\text{sq-2,4,5,6}) = \zeta(\text{sq-1,2,3,4,5}) \approx 46.86$, $\zeta(\text{sq-4,5,6}) = \zeta(\text{sq-1,3,4,5}) \approx 41.20$, $\zeta(\text{sq-2,5,6}) = \zeta(\text{sq-1,2,3,5}) \approx 28.97$, $\zeta(\text{sq-2,4,6}) = \zeta(\text{sq-1,2,3,4}) \approx 35.55$, $\zeta(\text{sq-5,6}) = \zeta(\text{sq-1,3,5}) \approx 23.31$, $\zeta(\text{sq-2,6}) = \zeta(\text{sq-1,2,3}) \approx 17.66$ and $\zeta(\text{sq-6}) = \zeta(\text{sq-1,3}) = 12$.

The differentiate power of a scalar index ζ is still better than the differentiate power of an index ξ and both are much better than the differentiate power of the total number of sites in the neighborhood z.

V. CONCLUSION

In this paper with Newman and Ziff effective Monte Carlo algorithm we calculated percolation thresholds for 32 complex neighbourhoods (containing sites from the sixth coordination zone) on a square lattice.

As scalar indexes ξ (5) and ζ (7) allow simultaneously to (more or less effective) distinguish between various neighbourhoods and accordingly fitting p_c to the inverse power-law on ξ (6) or ζ (8) (with various efficiency depending on the underlying lattice shape) searching for

another index remains an open task. The index may involve various powers of z_i, r_i and i, where i stands for the number of coordination zone from which sites constituting neighbourhood come from and z_i and r_i are the number and the distance of sites in this coordination zone to the central site in the neighbourhood, respectively.

Also calculating p_c for neighbourhoods containing sites up to the sixth coordination zone on triangular and honeycomb lattices seems to be desired. Simultaneous calculation of p_c for honeycomb and triangular lattices should allow for identifying inflated and equivalent neighbourhoods but among these two underlying regular lattices. Preliminary inspection of the $p_c(\zeta)$ dependence—but for neighbourhoods containing sites up to the fifth coordination zone [28]—reveals γ_2 close to $1/2$. This does not make factor ξ totally useless, as for the bond-percolation problem very clear dependnce (6) with $\gamma_1 \approx 1$ was recently observed [47].

Finally, the further studies may focus on the fractal nature of the giant component at $p = p_c$ [48]. The largest percolating cluster on square lattice at $p = p_c$ has fractal properties for SQ-1 neighbourhoods with fractal dimension close to 1.9 [14, p. 9]. Does this picture survive changing neighbourhoods to complex one, also on other lattice topologies? And if yes, is the fractal dimension the same as for the nearest-neighbours interactions?

The results obtained in this paper may be helpful in further searching for the universal formula, in the spirit of Equation (4) [49], for percolation threshold p_c, also for complex neighborhoods, but independently of the underlying two-dimensional lattice shape. Also further studies on the topic presented here may result in finding universal formula for p_c not only for two-dimensional lattices but in higher dimensions (including nonphysical dimensions, like on four- [34, 35] and five-dimensional simple hyper-cubic [50, 51] lattices).

Appendix A: Neighborhoods shapes

In Figure 4 the shapes of all complex neighborhoods containing sites from the sixth coordination zone are presented.

[1] S. R. Broadbent and J. M. Hammersley, "Percolation processes: I. Crystals and mazes," Mathematical Proceedings of the Cambridge Philosophical Society **53**, 629–641 (1957).

[2] J. M. Hammersley, "Percolation processes: II. The connective constant," Mathematical Proceedings of the Cambridge Philosophical Society **53**, 642–645 (1957).

[3] L. Cheng, P. Yan, X. Yang, H. Zou, H. Yang, and H. Liang, "High conductivity, percolation behavior and dielectric relaxation of hybrid ZIF-8/CNT composites," Journal of Alloys and Compounds **825**, 154132 (2020).

[4] Q. Zhang, B.-Y. Zhang, B.-H. Guo, Z.-X. Guo, and J. Yu, "High-temperature polymer conductors with self-assembled conductive pathways," Composites Part B—Engineering **192**, 107989 (2020).

[5] K. Malarz, S. Kaczanowska, and K. Kułakowski, "Are forest fires predictable?" International Journal of Modern Physics C **13**, 1017–1031 (2002).

[6] J. E. Ramírez, C. Pajares, M. I. Martínez, R. Rodríguez Fernández, E. Molina-Gayosso, J. Lozada-Lechuga, and A. Fernández Téllez, "Site-bond percolation solution to preventing the propagation of *Phytophthora zoospores* on plantations," Physical Review E **101**, 032301 (2020).

[7] B. Ghanbarian, F. Liang, and H.-H. Liu, "Modeling gas relative permeability in shales and tight porous rocks," Fuel **272**, 117686 (2020).

[8] R. M. Ziff, "Percolation and the pandemic," Physica A: Statistical Mechanics and its Applications **568**, 125723 (2021).

[9] S. Dong, A. Mostafizi, H. Wang, J. Gao, and X. Li, "Measuring the topological robustness of transportation networks to disaster-induced failures: A percolation approach," Journal of Infrastructure Systems **26**, 04020009 (2020).

[10] W. Cao, L. Dong, L. Wu, and Y. Liu, "Quantifying urban areas with multi-source data based on percolation theory," Remote Sensing of Environment **241**, 111730 (2020).

[11] S. Bartolucci, F. Caccioli, and P. Vivo, "A percolation model for the emergence of the Bitcoin Lightning Network," Scientific Reports **10**, 4488 (2020).

[12] M. Li, R.-R. Liu, L. Lü, M.-B. Hu, S. Xu, and Y.-C. Zhang, "Percolation on complex networks: Theory and application," Physics Reports **907**, 1–68 (2021).

[13] A. A. Saberi, "Recent advances in percolation theory and its applications," Physics Reports **578**, 1–32 (2015).

[14] D. Stauffer and A. Aharony, *Introduction to Percolation Theory*, 2nd ed. (Taylor and Francis, London, 1994).

[15] J. Wierman, "Percolation theory," in *Wiley StatsRef: Statistics Reference Online* (American Cancer Society, 2014) pp. 1–9.

[16] P. Dean, "A new Monte Carlo method for percolation problems on a lattice," Mathematical Proceedings of the Cambridge Philosophical Society **59**, 397–410 (1963).

[17] P. Dean and N. F. Bird, "Monte Carlo estimates of critical percolation probabilities," Mathematical Proceedings of the Cambridge Philosophical Society **63**, 477–479 (1967).

[18] P. N. Suding and R. M. Ziff, "Site percolation thresholds for Archimedean lattices," Physical Review E **60**, 275–283 (1999).

[19] N. W. Dalton, C. Domb, and M. F. Sykes, "Dependence of critical concentration of a dilute ferromagnet on the range of interaction," Proceedings of the Physical Society **83**, 496–498 (1964).

[20] C. Domb and N. W. Dalton, "Crystal statistics with long-range forces: I. The equivalent neighbour model," Proceedings of the Physical Society **89**, 859–871 (1966).

[21] M. Gouker and F. Family, "Evidence for classical critical behavior in long-range site percolation," Physical Review B **28**, 1449–1452 (1983).

[22] K. Malarz and S. Galam, "Square-lattice site percolation at increasing ranges of neighbor bonds," Physical Review E **71**, 016125 (2005).

[23] S. Galam and K. Malarz, "Restoring site percolation on damaged square lattices," Physical Review E **72**, 027103 (2005).

[24] M. Majewski and K. Malarz, "Square lattice site percolation thresholds for complex neighbourhoods," Acta Physica Polonica B **38**, 2191–2199 (2007).

[25] Z. Xun, D. Hao, and R. M. Ziff, "Site percolation on square and simple cubic lattices with extended neighborhoods and their continuum limit," Physical Review E **103**, 022126 (2021).

[26] C. d'Iribarne, M. Rasigni, and G. Rasigni, "From lattice long-range percolation to the continuum one," Physics Letters A **263**, 65–69 (1999).

[27] K. Malarz, "Site percolation thresholds on triangular lattice with complex neighborhoods," Chaos **30**, 123123 (2020).

[28] K. Malarz, "Percolation thresholds on triangular lattice for neighbourhoods containing sites up-to the fifth coordination zone," Physical Review E **103**, 052107 (2021).

[29] K. Malarz, "Random site percolation on honeycomb lattices with complex neighborhoods," Chaos **32**, 083123 (2022).

[30] W. Lebrecht, P. M. Centres, and A. J. Ramirez-Pastor, "Empirical formula for site and bond percolation thresholds on Archimedean and 2-uniform lattices," Physica A: Statistical Mechanics and its Applications **569**, 125802 (2021).

[31] Z. Xun, D. Hao, and R. M. Ziff, "Site and bond percolation thresholds on regular lattices with compact extended-range neighborhoods in two and three dimensions," Physical Review E **105**, 024105 (2022).

[32] Ł. Kurzawski and K. Malarz, "Simple cubic random-site percolation thresholds for complex neighbourhoods," Reports on Mathematical Physics **70**, 163–169 (2012).

[33] K. Malarz, "Simple cubic random-site percolation thresholds for neighborhoods containing fourth-nearest neighbors," Physical Review E **91**, 043301 (2015).

[34] M. Kotwica, P. Gronek, and K. Malarz, "Efficient space virtualisation for Hoshen–Kopelman algorithm," International Journal of Modern Physics C **30**, 1950055 (2019).

[35] P. Zhao, J. Yan, Z. Xun, D. Hao, and R. M. Ziff, "Site and bond percolation on four-dimensional simple hypercubic lattices with extended neighborhoods," Journal of Statistical Mechanics: Theory and Experiment **2022**, 033202 (2022).

[36] W. Xu, J. Wang, H. Hu, and Y. Deng, "Critical polynomials in the nonplanar and continuum percolation models," Physical Review E **103**, 022127 (2021).

[37] Z. Koza, G. Kondrat, and K. Suszczyński, "Percolation of overlapping squares or cubes on a lattice," Journal of Statistical Mechanics: Theory and Experiment **2014**, P11005 (2014).

[38] Z. Koza and J. Poła, "From discrete to continuous percolation in dimensions 3 to 7," Journal of Statistical Mechanics: Theory and Experiment **2016**, 103206 (2016).

[39] S. Galam and A. Mauger, "Universal formulas for percolation thresholds," Physical Review E **53**, 2177–2181 (1996).

[40] S. Galam and A. Mauger, "Reply to "Comment on 'Universal formulas for percolation thresholds'"," Physical Review E **55**, 1230–1231 (1997).

[41] S. C. van der Marck, "Universal formulas for percolation thresholds — Comment," Physical Review E **55**, 1228–1229 (1997).

[42] M. E. J. Newman and R. M. Ziff, "Fast Monte Carlo algorithm for site or bond percolation," Physical Review E **64**, 016706 (2001).

[43] V. Privman, "Finite-size scaling theory," in *Finite size scaling and numerical simulation of statistical systems*, edited by V. Privman (World Scientific, Singapore, 1990) pp. 1–98.

[44] D. P. Landau and K. Binder, *A Guide to Monte Carlo Simulations in Statistical Physics*, 3rd ed. (Cambridge University Press, 2009).

[45] M. E. J. Newman and R. M. Ziff, "Efficient Monte Carlo algorithm and high-precision results for percolation," Physical Review Letters **85**, 4104–4107 (2000).

[46] J. Tencer and K. M. Forsberg, "Postprocessing techniques for gradient percolation predictions on the square lattice," Physical Review E **103**, 012115 (2021).

[47] Z. Xun and D. Hao, "Monte Carlo simulation of bond percolation on square lattice with complex neighborhoods," Acta Physica Sinica **71**, 066401 (2022), in Chinese.

[48] M.-Á. M. Cruz, J. P. Ortiz, M. P. Ortiz, and A. Balankin, "Percolation on fractal networks: A survey," Fractal and Fractional **7**, 231 (2023).

[49] S. Galam and A. Mauger, "A new scheme to percolation thresholds," J. Appl. Phys. **75**, 5526–5528 (1994).

[50] S. Mertens and C. Moore, "Percolation thresholds and Fisher exponents in hypercubic lattices," Physical Review E **98**, 022120 (2018).

[51] Z. Xun, D. Hao, and R. M. Ziff, "Extended-range percolation in five dimensions," (2023), arXiv:2308.15719 [cond-mat.stat-mech].
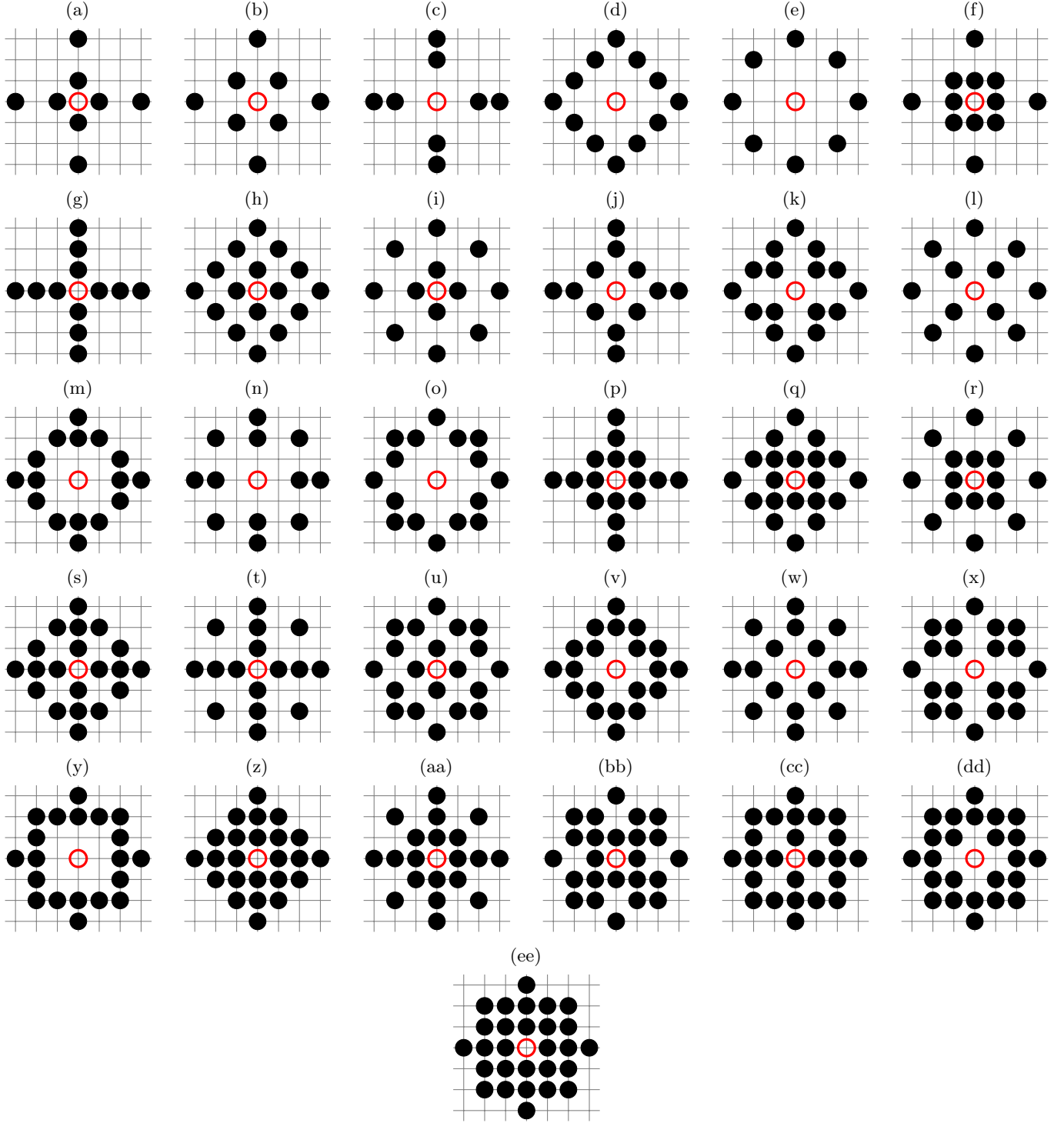
FIG. 4: Shapes of neighborhoods on square lattice combined with basics neighborhoods presented in Figure 1 and containing sites from the sixth coordination zone (Figure 1(f)). (a) sq-1,6, (b) sq-2,6, (c) sq-3,6, (d) sq-4,6, (e) sq-5,6, (f) sq-1,2,6, (g) sq-1,3,6, (h) sq-1,4,6, (i) sq-1,5,6, (j) sq-2,3,6, (k) sq-2,4,6, (l) sq-2,5,6, (m) sq-3,4,6, (n) sq-3,5,6, (o) sq-4,5,6, (p) sq-1,2,3,6, (q) sq-1,2,4,6, (r) sq-1,2,5,6, (s) sq-1,3,4,6, (t) sq-1,3,5,6, (u) sq-1,4,5,6, (v) sq-2,3,4,6, (w) sq-2,3,5,6, (x) sq-2,4,5,6, (y) sq-3,4,5,6, (z) sq-1,2,3,4,6, (aa) sq-1,2,3,5,6, (bb) sq-1,2,4,5,6, (cc) sq-1,3,4,5,6, (dd) sq-2,3,4,5,6, (ee) sq-1,2,3,4,5,6

SUPPLEMENTAL MATERIAL

Appendix A: Boundaries procedures

Below, we present a set of `boundaries()` functions (written in C) to be replaced in the Newman–Ziff program published in Reference 42 to obtain the single realization of $\mathcal{S}_{\max}(n; L)$ for the neighborhoods presented in Figures 1(a) to 1(f).

1. SQ-1

`boundaries()` function for the SQ-1 neighborhood (originally presented in Reference 42).

```
1  void boundaries()
2  {
3    int i,j;
4    for (i=0; i<N; i++) {
5  // 1nn core:
6      nn[i][0] = (N+i +1)%N;
7      nn[i][1] = (N+i -1)%N;
8      nn[i][2] = (N+i +L)%N;
9      nn[i][3] = (N+i -L)%N;
10 // 1nn left border:
11     if (i%L==0)     nn[i][1] = (N+i+L -1)%N;
12 // 1nn right border:
13     if ((i+1)%L==0) nn[i][0] = (N+i-L +1)%N;
14   }
15 }
```

2. SQ-2

`boundaries()` function for the SQ-2 neighborhood.

```
1  void boundaries()
2  {
3    int i,j;
4    for (i=0; i<N; i++) {
5  // 2nn core:
6      nn[i][0] = (N+i +L+1)%N;
7      nn[i][1] = (N+i +L-1)%N;
8      nn[i][2] = (N+i -L+1)%N;
9      nn[i][3] = (N+i -L-1)%N;
10 // 2nn left border:
11     if(i%L==0) {
12        nn[i][1] = (N+i+L +L-1)%N;
13        nn[i][3] = (N+i+L -L-1)%N; }
14 // 2nn right border:
15     if((i+1)%L==0) {
16        nn[i][0] = (N+i-L +L+1)%N;
17        nn[i][2] = (N+i-L -L+1)%N; }
18   }
19 }
```

3. SQ-3

`boundaries()` function for the SQ-3 neighborhood.

```
1  void boundaries()
2  {
3    int i,j;
4    for (i=0; i<N; i++) {
5  // 3nn core:
6      nn[i][0] = (N+i +2*L)%N;
7      nn[i][1] = (N+i -2*L)%N;
8      nn[i][2] = (N+i +2)%N;
9      nn[i][3] = (N+i -2)%N;
10 // 3nn left border:
11     if(i%L==0 || i%L==1)
12        nn[i][3] = (N+i+L -2)%N;
13 // 3nn right border:
14     if((i+1)%L==0 || (i+2)%L==0)
15        nn[i][2] = (N+i-L +2)%N;
16   }
17 }
```

4. SQ-4

`boundaries()` function for the neighborhood SQ-4. The preprocesor directive `#define Z 4` in source code in Reference 42 requires replacing to `#define Z 8`.

```
1  void boundaries()
2  {
3    int i,j;
4    for (i=0; i<N; i++) {
5  // 4nn core:
6      nn[i][0] = (N+i +L+2)%N;
7      nn[i][1] = (N+i +L-2)%N;
8      nn[i][2] = (N+i -L+2)%N;
9      nn[i][3] = (N+i -L-2)%N;
10     nn[i][4] = (N+i +2*L+1)%N;
11     nn[i][5] = (N+i +2*L-1)%N;
12     nn[i][6] = (N+i -2*L+1)%N;
13     nn[i][7] = (N+i -2*L-1)%N;
14 // 4nn left border:
15     if(i%L==0 || i%L==1 ) {
16        nn[i][1] = (N+i+L +L-2)%N;
17        nn[i][3] = (N+i+L -L-2)%N;
18        nn[i][5] = (N+i+L +2*L-1)%N;
19        nn[i][7] = (N+i+L -2*L-1)%N; }
20 // 4nn right border:
21     if((i+1)%L==0 || (i+2)%L==0) {
22        nn[i][0] = (N+i-L +L+2)%N;
23        nn[i][2] = (N+i-L -L+2)%N;
24        nn[i][4] = (N+i-L +2*L+1)%N;
25        nn[i][6] = (N+i-L -2*L+1)%N; }
26   }
27 }
```

5. SQ-5

`boundaries()` function for the SQ-5 neighborhood.

```
1  void boundaries()
2  {
3    int i,j;
4    for (i=0; i<N; i++) {
5  // 5nn core:
6      nn[i][0] = (N+i +2*L+2)%N;
7      nn[i][1] = (N+i +2*L-2)%N;
8      nn[i][2] = (N+i -2*L+2)%N;
9      nn[i][3] = (N+i -2*L-2)%N;
10 // 5nn left border:
11     if(i%L==0 || i%L==1) {
```

```
12        nn[i][1]  = (N+i+L +2*L-2)%N;
13        nn[i][3]  = (N+i+L -2*L-2)%N; }
14 // 5nn right border:
15    if((i+1)%L==0 || (i+2)%L==0) {
16        nn[i][0]  = (N+i-L +2*L+2)%N;
17        nn[i][2]  = (N+i-L -2*L+2)%N; }
18   }
19 }
```

```
8      nn[i][2]  = (N+i +3)%N;
9      nn[i][3]  = (N+i -3)%N;
10 // 6nn left border:
11    if(i%L==0 || i%L==1 || i%L==2)
12        nn[i][3]  = (N+i+L -3)%N;
13 // 6nn right border:
14    if((i+1)%L==0 || (i+2)%L==0 || (i+3)%L==0)
15        nn[i][2]  = (N+i-L +3)%N;
16   }
17 }
```

6. SQ-6

`boundaries()` function for the sq-6 neighborhood.

```
1 void boundaries()
2 {
3   int i,j;
4   for (i=0; i<N; i++) {
5 // 6nn core:
6       nn[i][0]  = (N+i +3*L)%N;
7       nn[i][1]  = (N+i -3*L)%N;
```

Appendix B: Dependencies of $\mathcal{P}_{\max} \cdot L^{\beta/\nu}$ on the probability of occupation p

Figure 5 presents the dependencies of $\mathcal{P}_{\max} \cdot L^{\beta/\nu}$ on the probability of occupation p for neighborhoods ranging from sq-6 to sq-1,2,3,4,5,6 for various linear system sizes $L = 128, 256, 512, 1024, 2048$, and 4096.
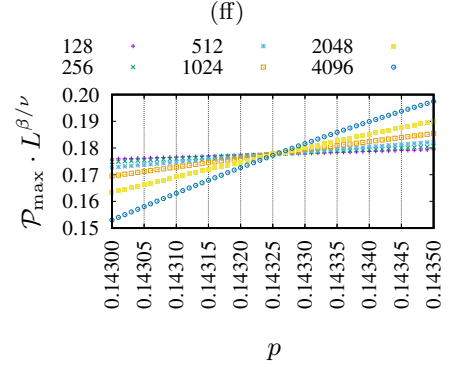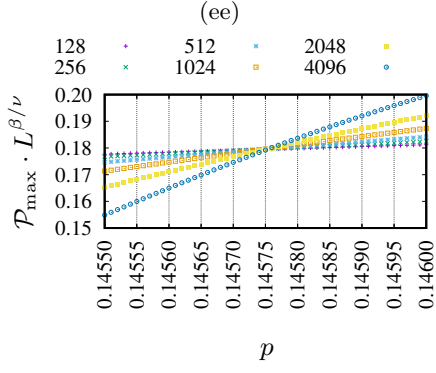
(a) (b) (c)

(d) (e) (f)

(g) (h) (i)

(j) (k) (l)

(m) (n) (o)
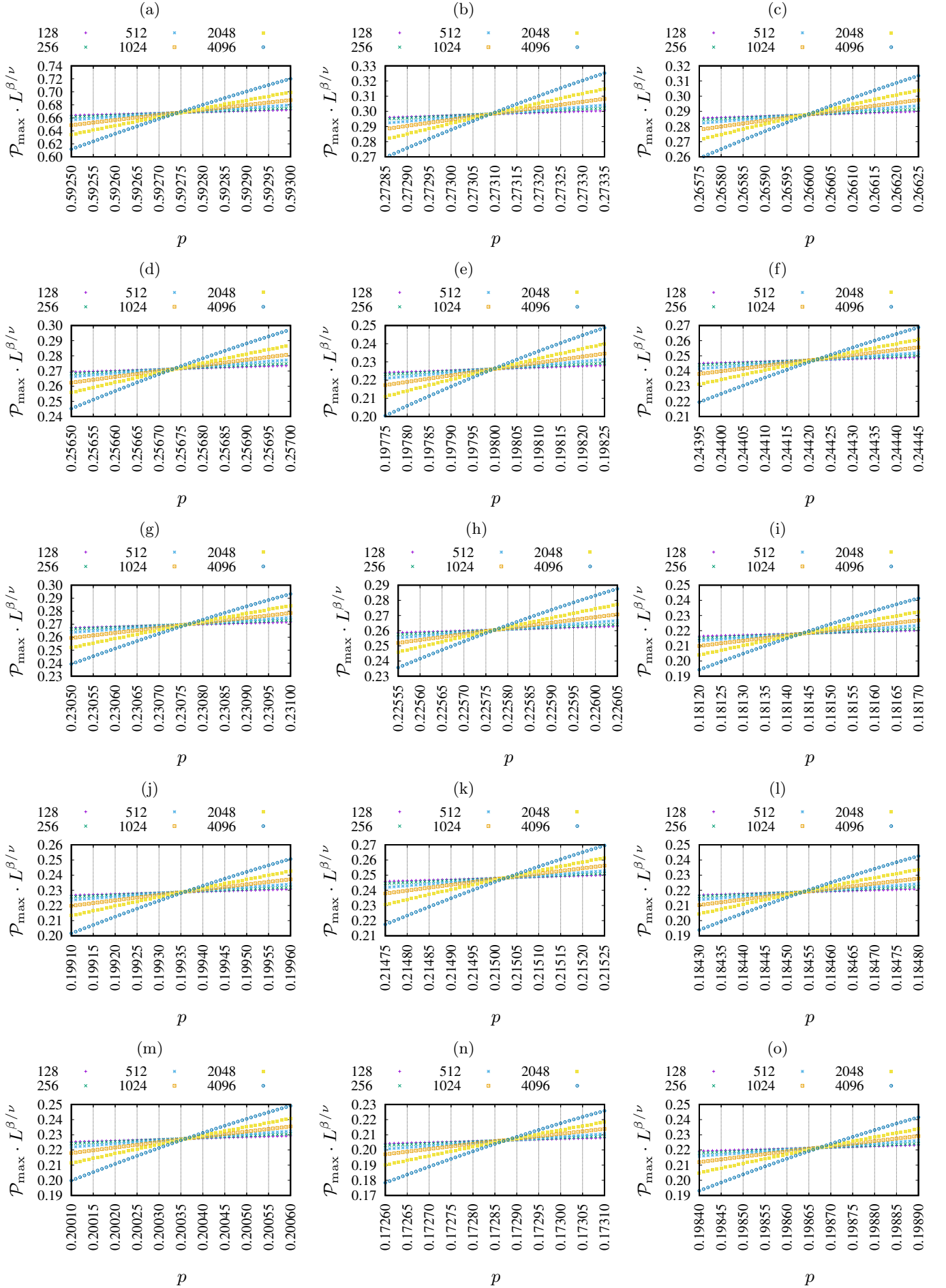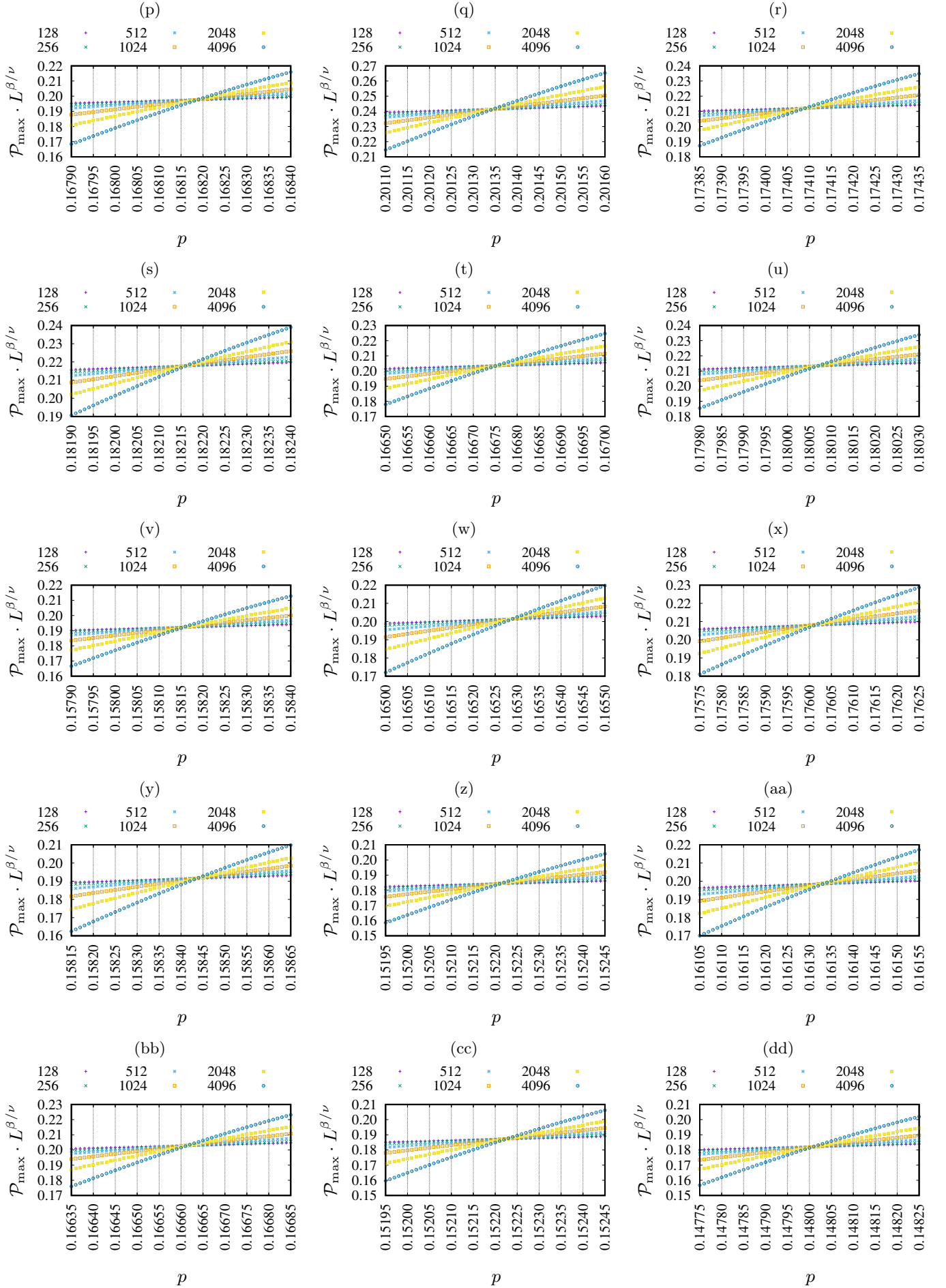
FIG. 5: $L^{\varepsilon_1}\mathcal{P}_{\max}$ vs. p for various complex neighborhoods and various values of L indicated in the title of the figures. The results are averaged over the realizations of the $R = 10^5$ system. The probability of occupation p is scanned with $\Delta p = 10^{-5}$ separation step. (a) sq-6, (b) sq-1,6, (c) sq-2,6, (d) sq-3,6, (e) sq-4,6, (f) sq-5,6, (g) sq-1,2,6, (h) sq-1,3,6, (i) sq-1,4,6, (j) sq-1,5,6, (k) sq-2,3,6, (l) sq-2,4,6, (m) sq-2,5,6, (n) sq-3,4,6, (o) sq-3,5,6, (p) sq-4,5,6, (q) sq-1,2,3,6, (r) sq-1,2,4,6, (s) sq-1,2,5,6, (t) sq-1,3,4,6, (u) sq-1,3,5,6, (v) sq-1,4,5,6, (w) sq-2,3,4,6, (x) sq-2,3,5,6, (y) sq-2,4,5,6, (z) sq-3,4,5,6, (aa) sq-1,2,3,4,6, (bb) sq-1,2,3,5,6, (cc) sq-1,2,4,5,6, (dd) sq-1,3,4,5,6, (ee) sq-2,3,4,5,6, (ff) sq-1,2,3,4,5,6